51th Fluid Dynamics Conference / 37th Aerospace Numerical Simulation Symposium
1 July 2019

FaSTARによる
各種乱流モデルを用いた30P30Nの解析

Computation of 30P30N in Various Turbulence Models by FaSTAR Code

TAKEDA Hisato, YAMAMOTO Takahiro, HAYASHI Kenji
(Ryoyu Systems Co., Ltd.)

ISHIDA Takashi, SAKAI Ryotaro
HASHIMOTO Atsushi, AOYAMA Takashi
(JAXA)

1

Case 1-1 Calculation method

➢ Flow solver : FaSTAR

- Grid : Provided
  - 2D (L2)
  - 30P30N
- Steady calculation
- Discretization : Cell-Center
- Inviscid flux : SLAU
- Reconstruction : U-MUSCL
- Gradient : GLSQ
- Slope limiter : Hishida (van Lee-type)
- Time integration ： LU-SGS
- Boundary Conditions
  - Spanwise direction : Periodic
  - Wall surfaces : No-slip

➢ Turbulence models

- ☐ SA
- ☐ SAR (C_{rot}=1, r_{mod}) : FaSTAR
- ☐ SAR (C_{rot}=2, r_{ori}) : Reference
- ☐ SAR (C_{rot}=1, r_{ori})
- ☐ SAR (C_{rot}=2, r_{mod})
- ☐ SARC
- ☐ SST
- ☐ SSTV
- ☐ SST-2003
- ☐ SST-2003sust
- ☐ EARSM

2

Turbulence model

One equation model

- SA-noft2

$$\frac{\partial \rho \hat{v}}{\partial t}+\frac{\partial \rho \hat{v} u_j}{\partial x_j}=\rho C_{b1}\hat{S}\hat{v}-\rho C_{w1}f_w\left(\frac{\hat{v}}{d}\right)^2+\frac{\partial}{\partial x_j}\left(\frac{\rho}{\sigma}(v+\hat{v})\frac{\partial \hat{v}}{\partial x_j}\right)+\rho\frac{C_{b2}}{\sigma}\frac{\partial \hat{v}}{\partial x_i}\frac{\partial \hat{v}}{\partial x_i}$$

- SA-noft2-R

  - Production term $\hat{S}=\Omega+\frac{\hat{v}}{\kappa^2 d^2}f_{v2}$ → $\hat{S}_R=\Omega+C_{rot}min(0,S-\Omega)+\frac{\hat{v}}{\kappa^2 d^2}f_{v2}$

  - Destruction term $f_w=f(r)$ $\quad r_{ref}=\frac{\hat{v}}{max(\hat{S}\kappa^2 d^2,\varepsilon)}$ $\quad r_{FaS}=\frac{\hat{v}}{max(\hat{S}_R\kappa^2 d^2,\varepsilon)}$

μ_t decrease (→)

μ_t decrease (↓)

	$C_{rot}=1$	$C_{rot}=2$
r_{ref}	μ_t_max	Reference
r_{FaS}	FaSTAR	μ_t_min

- SA-noft2-RC

  - Rotation and curvature effects are added in SA-noft2 model

  - Production term $\quad c_{b1}\hat{S}\hat{v}\rightarrow c_{b1}\hat{S}\hat{v}f_{r1}$

3

Turbulence model

Tow equation model

- SST model

  - Standard Menter SST model

  - Production term

$$P_k=\frac{M_\infty}{Re_\infty}\mu_t\left[S^2-\frac{2}{3}\left(\frac{\partial u_k}{\partial x_k}\right)^2-\frac{2}{3}\rho k\frac{\partial u_k}{\partial x_k}\right]$$

- SSTV model

  - Production term

$$P_k=\frac{M_\infty}{Re_\infty}\mu_t\Omega^2-\frac{2}{3}\rho k\frac{\partial u_t}{\partial x_k}$$

- SST-2003 model

  - Menter SST from 2003 model (production term : strain rate)

$$\mu_t=\frac{\rho a_1 k}{max\left(a_1\omega,\frac{M_\infty}{Re_\infty}\Omega F_2\right)}\rightarrow\mu_t=\frac{\rho a_1 k}{max\left(a_1\omega,\frac{M_\infty}{Re_\infty}SF_2\right)}$$

- SST-2003sust model

  - Sustaining term is added for preventing unphysical decay of turbulence statistics at external flow

4

Aerodynamic coefficients

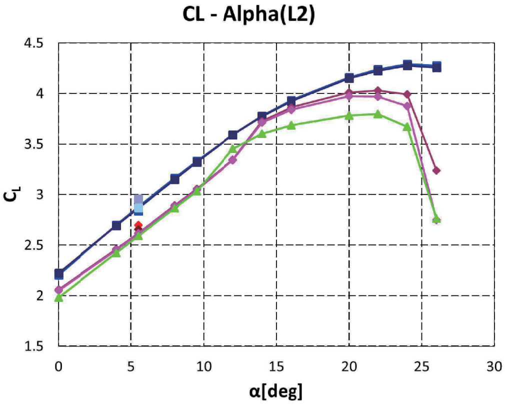

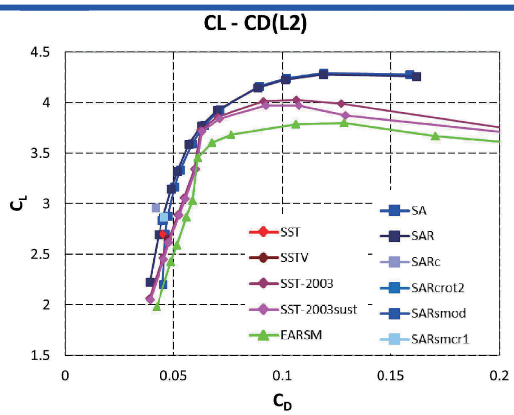

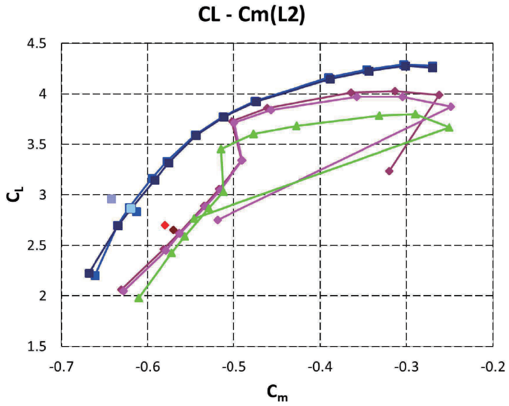

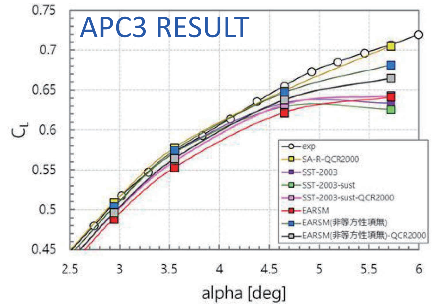

- Stall is observed in case of SST models.
- Characteristics of turbulence models are shown.

5

Comparison of Cp

Comparison of C_p in all calculation conditions

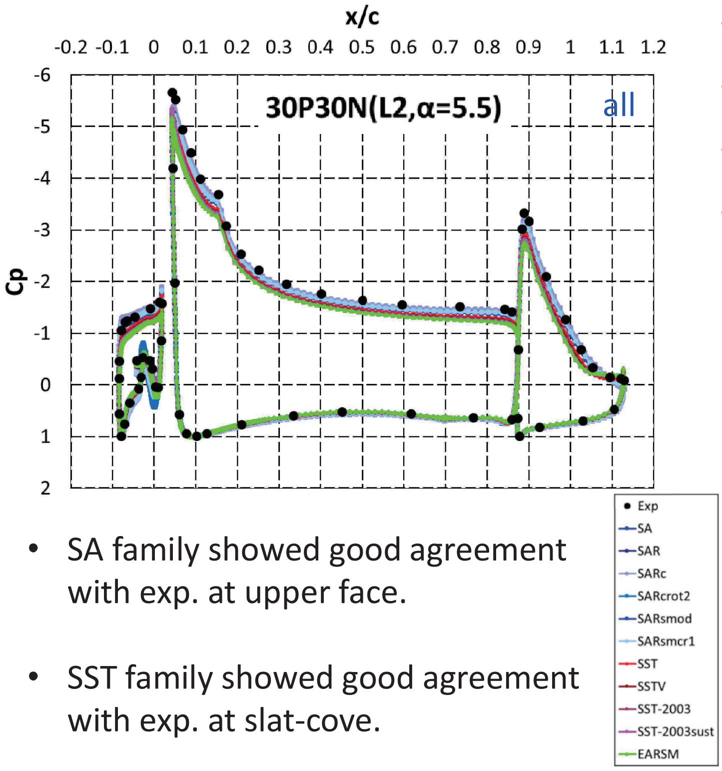

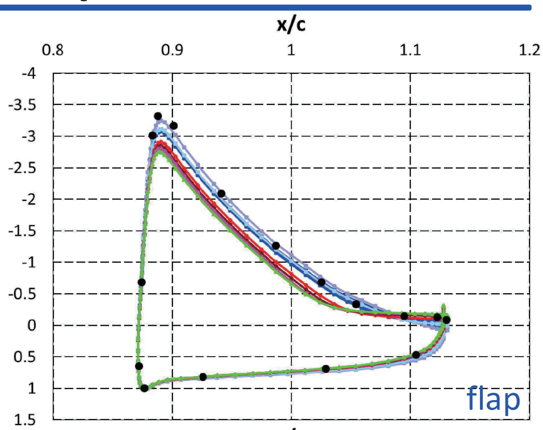

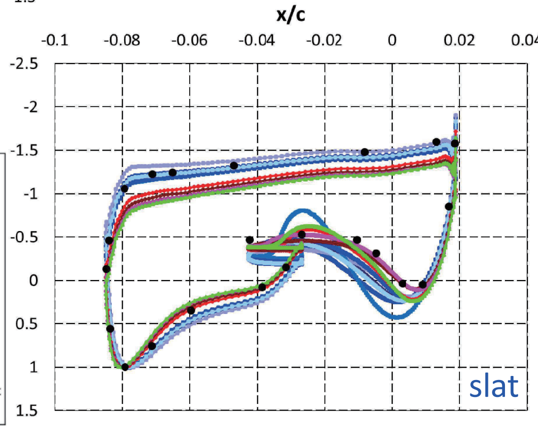

- SA family showed good agreement with exp. at upper face.
- SST family showed good agreement with exp. at slat-cove.

6

Comparison of flow field

Mach Number SAR SST-2003sust EARSM

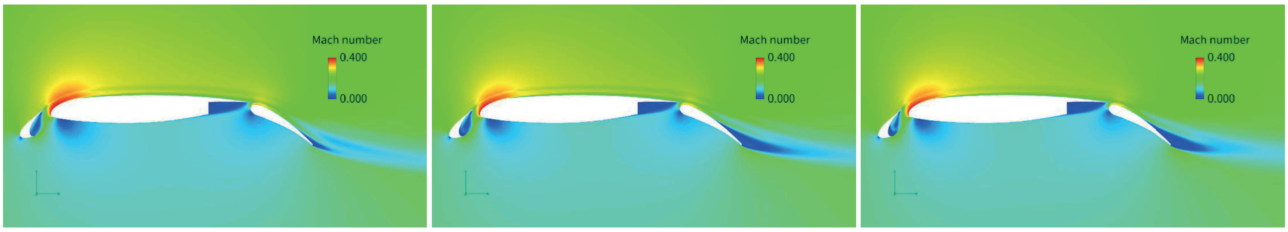

Turbulent viscosity ratio

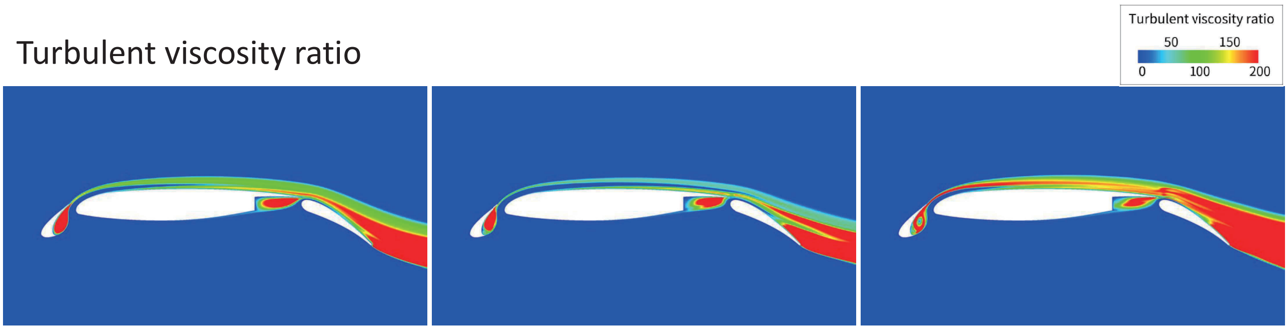

- The difference between one and two equation model is observed at slat and flap.
- Two equation model seems to overestimate flow separation at flap.

CD of each parts

L2, AOA = 5.5 deg

Flap

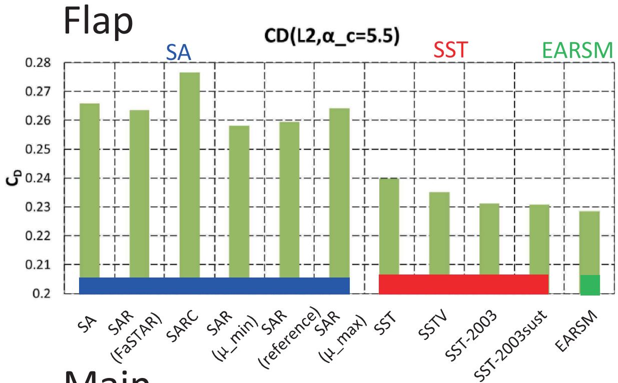

Slat

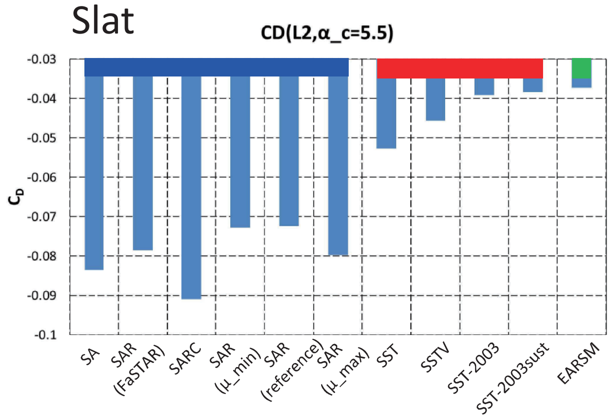

Main

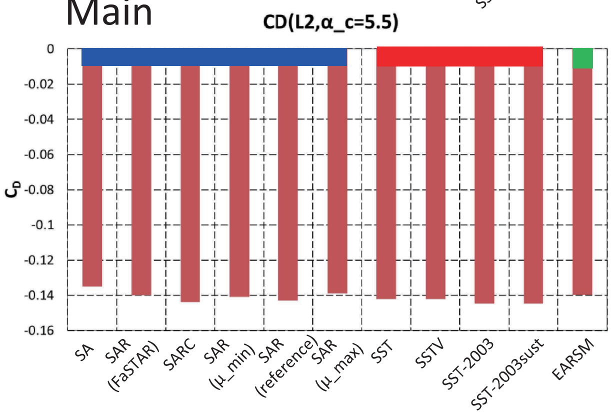

- Each turbulence model predicted different CD.

- SA predicted higher CD at Flap and Slat than other models.

Turbulent viscosity ratio : SA

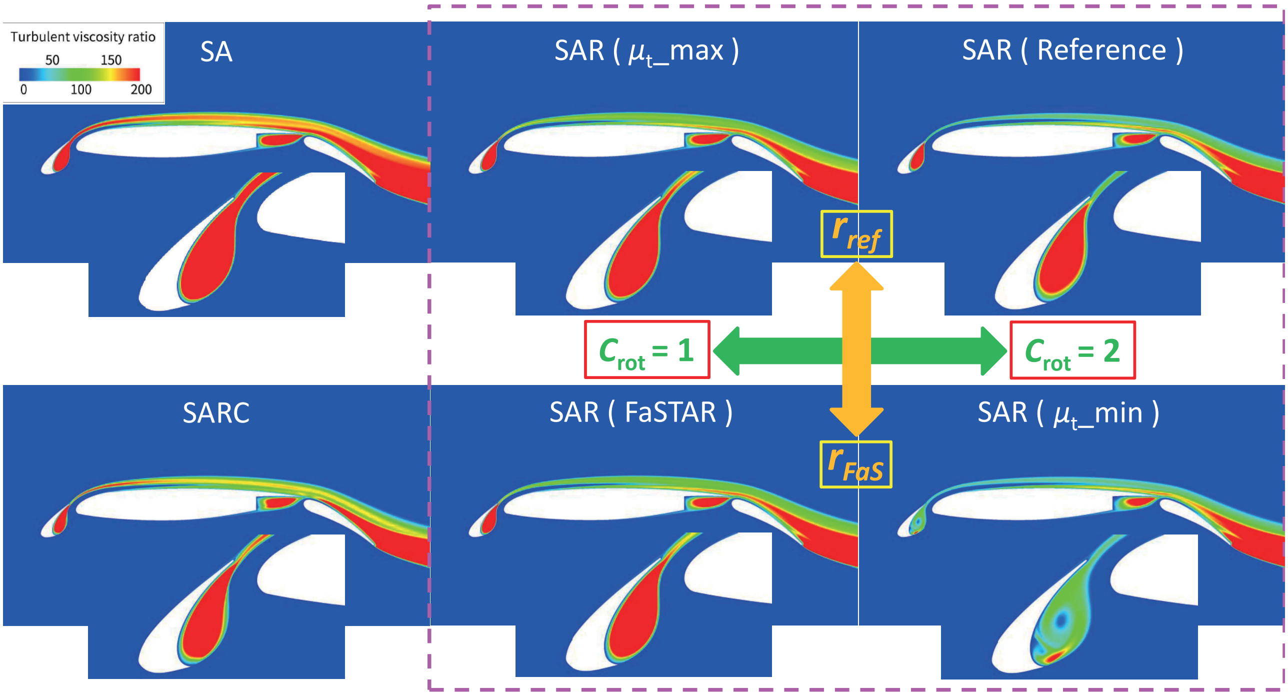

- Modification of C_{rot} and destruction term r have large influence on turbulent viscosity at slat-cove.

9

Turbulent viscosity ratio : SST

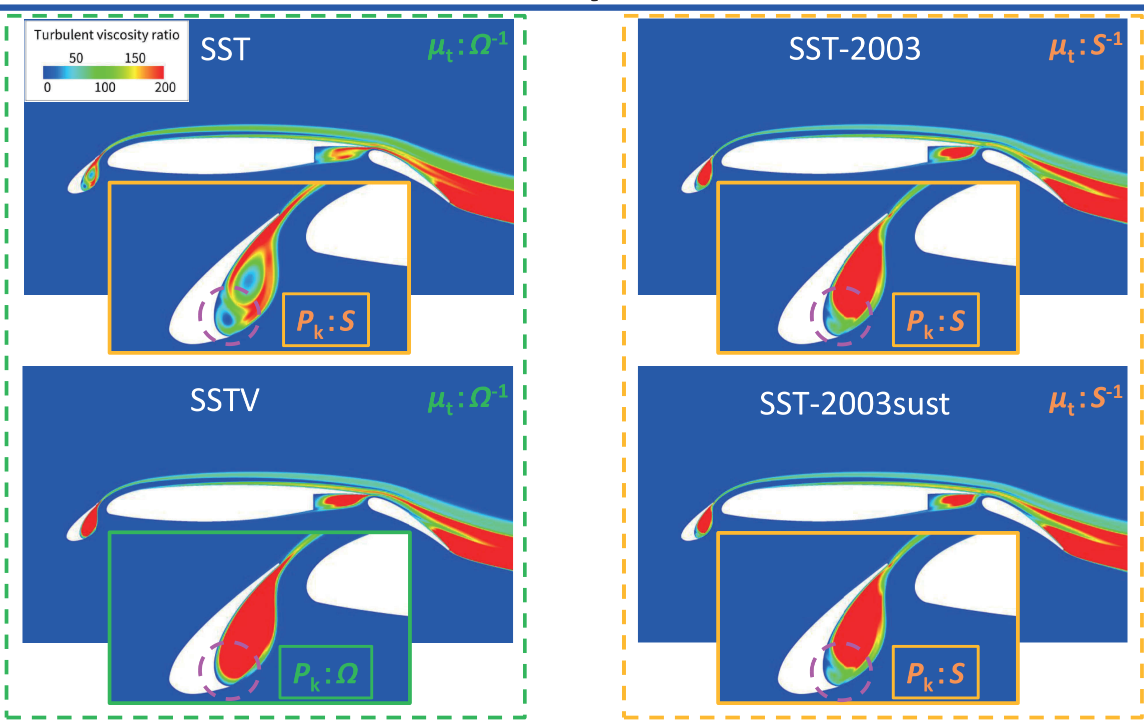

Vorticity is larger than strain rate at slat-cove.

- Production term determines the tendency depending on whether the evaluation is S or Ω.
- SST-2003 improves turbulent viscosity compared with standard SST.

10

Case 3 Calculation method

- Flow solver : FaSTAR
  - Grid : Provided
    - 2.5D (L2)
    - 30P30N
  - Unteady calculation
  - Discretization : Cell-Center
  - Inviscid flux : SLAU
  - Reconstruction : U-MUSCL
  - Gradient : GLSQ
  - Slope limiter : Hishida (vL)
  - Time integration ： LU-SGS
  - Boundary Conditions
    - Span wise and surfaces : Periodic
  - Turbulence model : SA-noft2-R
    SST-2003sust
    - Unsteady : DDES
  - Angle of Attack : 5.5 deg

11

Comparison of flow field

SADDES | SST-2003sust DDES

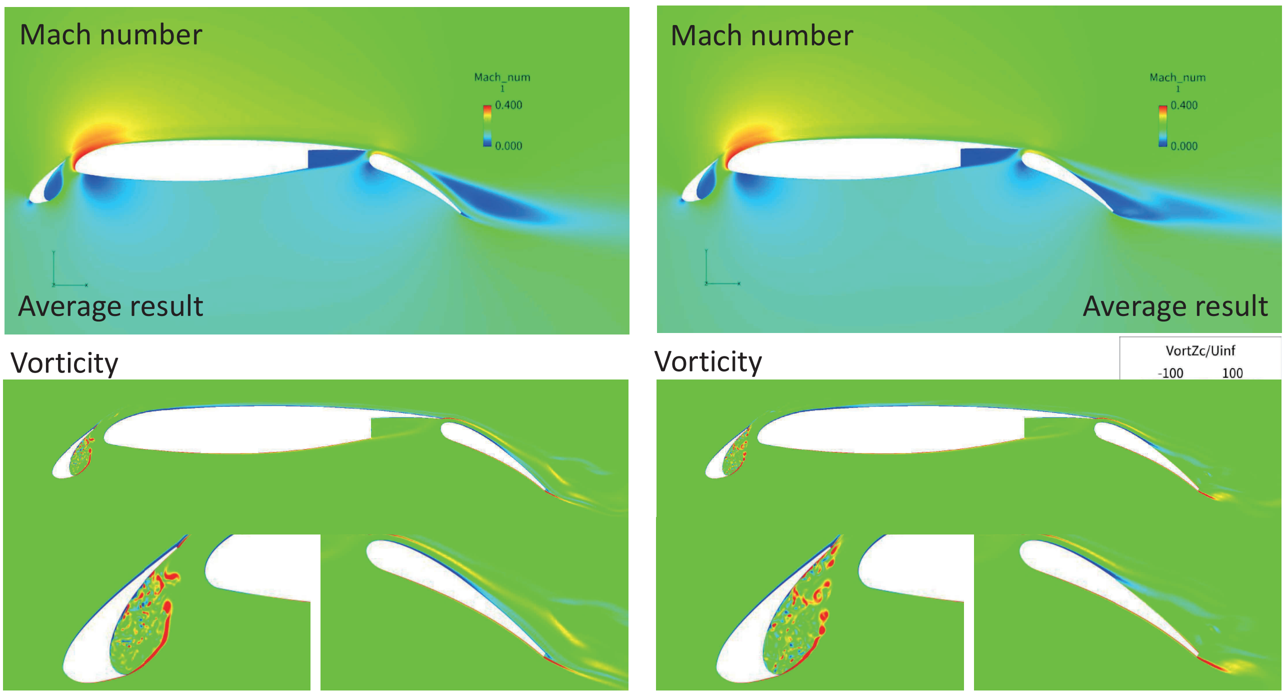

SST-2003sust DDES model, separation is observed at flap. On the other hand, there is not separation at same region in case of analysis using SADDES model.

12

PSD & Coherence

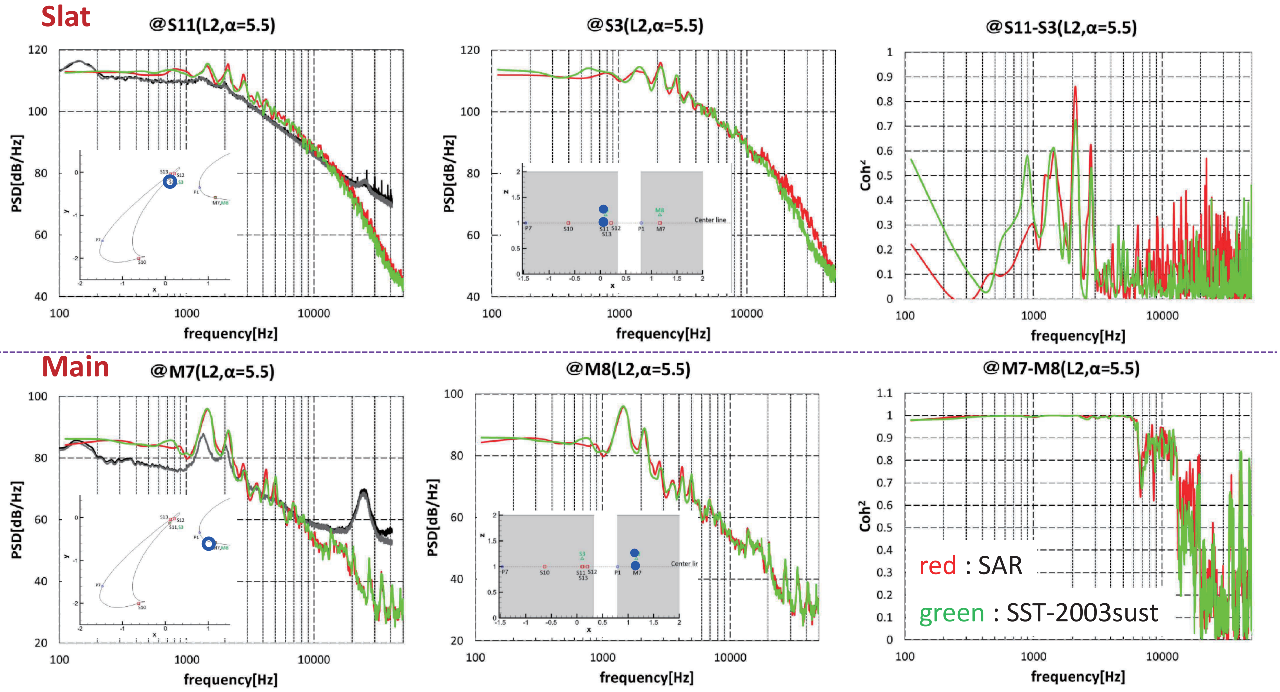

- PSD and coherence of surface pressure do not affected by turbulence model.
- Peak position and value of PSD correspond to experimental result roughly.
  → Because of coarse mesh.

13

Length scale of DDES

Compared with length scale of DDES.

Definition of DDES scale $L_{DDES} = L_{RANS} - f_d \, max(0, L_{RANS} - L_{LES})$

$\because f_d = 1 - tanh[(C_{dl} r_d)^3]$

L2 : FaSTAR	L2 : dmax (mesh length)
$\Delta = min[max(C_{wall} d, C_{wall} \Delta_{max}, \Delta_{wn}), \Delta_{max}]$ $\because C_s = 0.2, C_{wall} = 0.15$ $\quad d = wall\ length$ $\Delta_{wn} = min(\Delta x, \Delta y, \Delta z)$	$\Delta = \Delta_{max} = max(\Delta x, \Delta y, \Delta z)$ $\because \Delta x, \Delta y, \Delta z$: cell spacing in each coordinate directions.

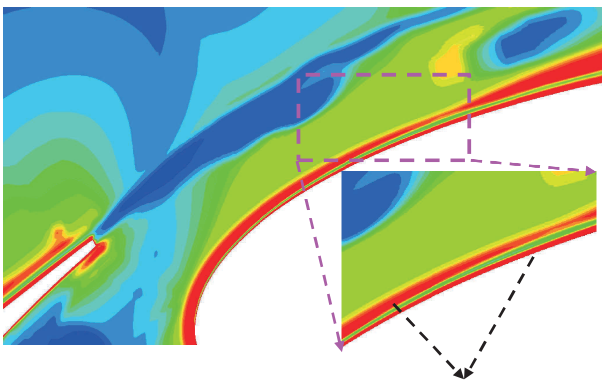

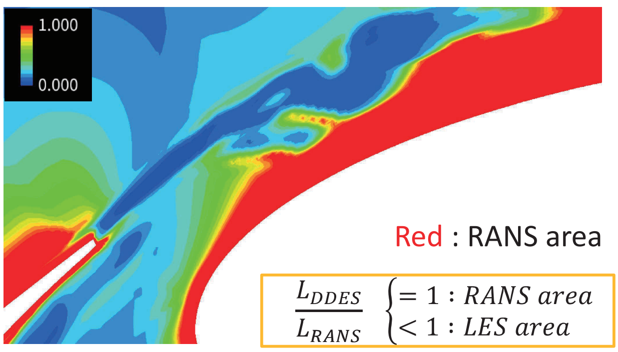

Red : RANS area

$$\frac{L_{DDES}}{L_{RANS}} \begin{cases} = 1 : RANS\ area \\ < 1 : LES\ area \end{cases}$$

SADDES

Distribution of RANS area is layered.

14

RMS of C_p (length scale of DDES)

SA-noft2-R DDES

The influence of length scale is confirmed by observing RMS of *C*p.
RMS of C_p distributions calculated by several length scale of DDES around Slat region are shown below.

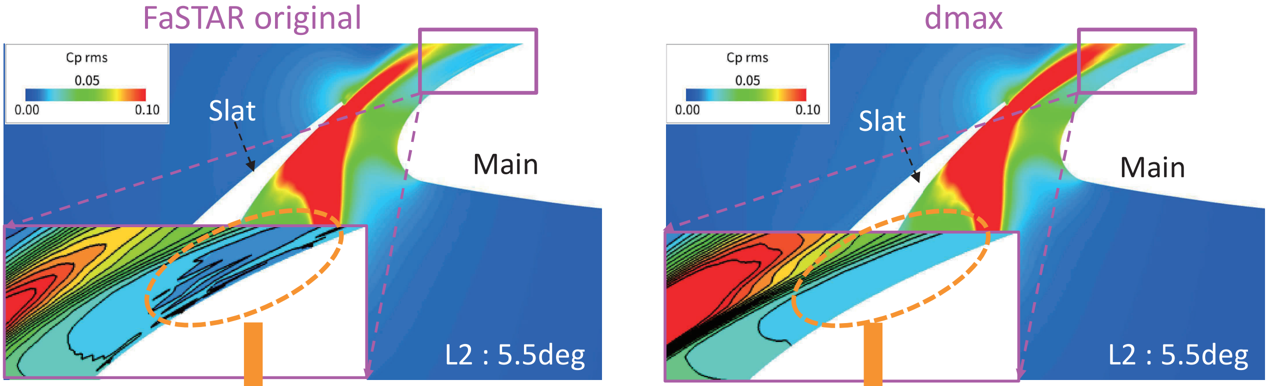

Anomaly distribution of C_p RMS occurs at the leading edge of Main.

Unphysical phenomenon does not exist.

- It is confirmed that length scale of DDES influences RMS of C_p.

15

Comparison of PSD

PSD (FaSTAR original) and PSD (dmax) are compared in both near and far field.

Red : FaSTAR
Green : dmax

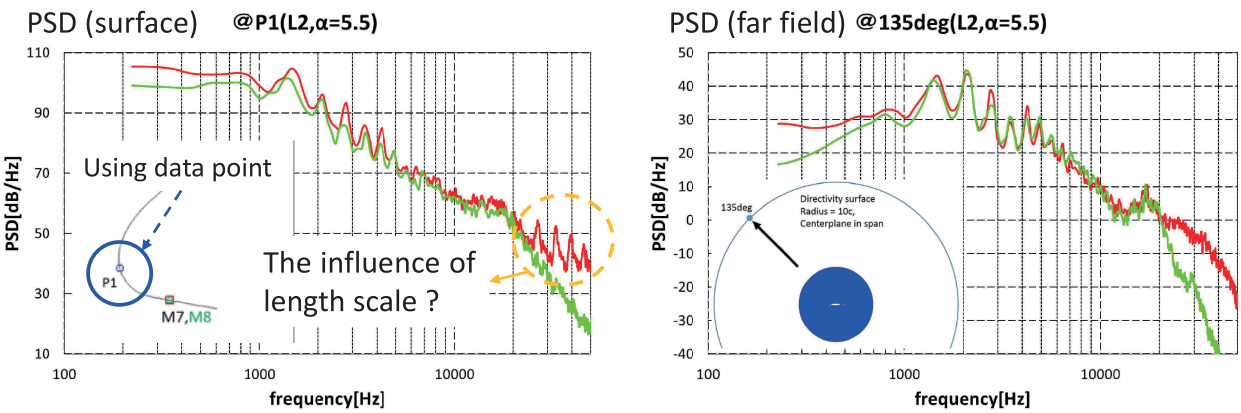

Both PSD is similar position of peaks and values.

Both PSD is similar position of peaks and values at the low frequency region.

- It seems that length scale of DDES does not influence PSD in low frequency area.

16

Summary

➢ Difference of various turbulence model in 2D (30P30N)

■ Each turbulence model group

- Characteristics of turbulence models were shown.
- Relatively large flow separation around flap was observed in case of SST models.
- The region where C_p corresponds to experimental data was changed by turbulence model.

■ In same turbulence model group

SA group

- Above Main region, modification of C_{rot} tends to influence turbulence viscosity largely.
- Around Slat region, modification of destruction term *r* tends to have an effect on turbulence viscosity mainly.

SST group

- Turbulence viscosity is more grown by production term defined by vorticity than by turbulence viscosity defined by strain rate.

Summary

➢ Difference of various turbulence model in 3D (30P30N)

- In case of using SST-2003sust DDES model, large flow separation was observed at flap.
- Peak position and coherence of PSD does not depend on each turbulence models.
- PSD was similar to experimental result roughly.

➢ Compared with length scale

- It was observed that distribution of RANS area is layered.
- Length scale of DDES did not influence PSD in low frequency area.